JMEPEG (2011) 20:591–596
DOI: 10.1007/s11665-010-9792-0

1059-9495/$19.00

Nitinol Fatigue Investigation on Stent-Finish Specimens Using Tension-Tension Method

Z. Lin, K. Pike, A. Zipse, and M. Schlun

(Submitted July 15, 2010; in revised form November 12, 2010)

Nitinol fatigue strain limit versus both strain amplitude (range 0.25-1.25%) and mean strain (1.0, 2.0, and 4.0%) was investigated using a tension-tension method. In order to apply the fatigue testing results to a nitinol stent and evaluate stent fatigue performance, the dog-bone style specimens were processed from the same raw material common to implantable stent manufacturing, i.e., similar nitinol tubing, surface quality, and electropolished surface. To simulate a physiological environment, the tension-tension fatigue tests were conducted in water at 37 °C. This strain-controlled fatigue test was conducted with a run-out set at 10^6 cycles. The fatigue strain limit at 10^6 cycles as well as the mean strain effect and the effects of inclusions are discussed. Fatigue results appeared in a bi-modal pattern when the strain amplitude was at a level between too high, which made all specimens to fail, and too low, which allowed all specimens to survive.

Keywords failure analysis, fatigue, mean strain, nitinol, strain amplitude

1. Introduction

Nitinol superelasticity has found its applications as a material for vascular devices (Ref 1). Many studies on nitinol fatigue resistance used sub-size specimens (Ref 2-4). A few of the factors that were discussed, which could impact testing and evaluation of nitinol fatigue behavior are (1) strain and stress; (2) the mode of applied loading such as bending or tension; (3) testing conditions, such as media temperature, testing speed, and transformation temperatures; (4) material inclusion; (5) the surface quality of the specimen; and (6) specimen design and dimension control. Researchers are still debating on the mechanism of nitinol fatigue behavior. The key questions of the debate are: what is the fatigue limit for nitinol? and how mean strain affects nitinol fatigue resistance?

In previous studies using tension-tension method, Tabanli et al. (Ref 5) tested nitinol tubing for fatigue strain limit versus different mean strains and strain amplitudes. The test method employed was tension-tension, and the results showed that fatigue resistance was greater when nitinol fatigues in a strain range within a single phase than that when it fatigues in a strain range of austenite and martensite coexisting phases.

The purpose of this study is to determine nitinol fatigue strain limit as a function of mean strain and strain amplitude in the range up to 10^6 cycles. Efforts have been made to freeze variations of specimen such as surface finish and design. The specimen surface has a stent-like finish with tight dimension control (coefficients of variation on strut width and thickness are 3.2 and 2.5%, respectively). Two reasons for adopting a standard tension-tension micro dog-bone style specimen are (1) no need to introduce a model to calculate global strain—it is simply equal to the deformation divided by the gage length; and (2) worst case scenario—maximum strain is distributed along the gage length and specimen's cross section.

Z. Lin and **K. Pike**, Abbott Vascular, Santa Clara, CA; and **A. Zipse** and **M. Schlun**, Bard Peripheral Vascular, Karlsruhe, Germany. Contact e-mail: zhicheng.lin@av.abbott.com.

2. Experimental

2.1 Specimen Preparation

The dog-bone style specimens were prepared by processing the specimen in a similar method as a stent:

(1) Design dog-bone stent cage that connects four dog-bone style specimens as shown in Fig. 1.
(2) Laser-cut the stent cage with nitinol hypotube.
(3) Heat-expand the stent cage to a diameter of 12 mm (the A_f of the dog-bone was 22 ± 2 °C as determined by Differential Scanning Calorimetry).
(4) Electropolish the expanded stent—a typical surface finish of the dog-bone specimen after electropolishing is shown in Fig. 2.
(5) Conduct inspection and separate the dog-bone style specimens from the stent cage.

The dimensions are measured at the gage section. The tolerances of both strut width and strut thickness are listed in Table 1.

2.2 Testing Method

Before carrying out the fatigue test, each dog-bone style specimen was subjected to pre-straining by loading it to a

strain of 8% and then unloading. The preconditioning simulated a stent collapse into a delivery catheter. The fatigue test setup is shown in Fig. 3. The maximum (peak) and minimum (valley) strain and stress were recorded for the test. The test was strain controlled, but the peak and valley stresses were also recorded for two purposes: (1) monitoring anomalies, such as grip slippage, drift, or outliers; and (2) determining the cycle number when the specimen breaks. The fatigue testing was set at 20 Hz, and the medium was 37 °C distilled water. The run-out of the fatigue test was set to 10^6 cycles. The specimens were fatigued at different levels of strain amplitude ε_a and mean strain ε_m as indicated in Table 2. Some strain levels have greater sample size because of the bimodal response. The ε_m and ε_a were determined per following formulas:

$$\varepsilon_m = \frac{\varepsilon_{max} + \varepsilon_{min}}{2} \quad \text{(Eq 1)}$$

$$\varepsilon_a = \frac{\varepsilon_{max} - \varepsilon_{min}}{2} \quad \text{(Eq 2)}$$

$$\varepsilon_{max} = \frac{(L_{peak} - L_o)}{L_g} \times 100\% \quad \text{(Eq 3)}$$

$$\varepsilon_{min} = \frac{(L_{valley} - L_o)}{L_g} \times 100\% \quad \text{(Eq 4)}$$

where L_o is the gap between upper and lower grips when the test specimen is in its natural position (a fixed value of 25 mm in this study), and L_{peak} and L_{valley} are, respectively, the maximum and minimum gaps between grips during a fatigue test. The values of L_{peak} and L_{valley} are inputs to obtain different strain settings. The input values were validated using a LVDT to verify the coordinate outputs. L_g is the gage length of the fatigue test specimens (a fixed value of 20 mm for this dog-bone specimen design).

3. Results

Fatigue strain limit is plotted as a function of both strain amplitude and mean strain as shown in Fig. 4. Data points of the fatigue test are listed in Table 3. Fatigue resistance, which was measured as cycle number to failure, decreases when increasing the strain amplitude. The results indicate the best fatigue resistance at a mean strain of 1.0%. The change in fatigue resistance is minimal with mean strain values ranging between 2.0 and 4.0%, especially when strain amplitude was 1.0% or below.

The probability of fracture (P) is introduced to compare the differences in fatigue resistance between different mean strains and strain amplitudes. The comparison of probability was conducted for all different levels of strain amplitude. Therefore, it helps us to understand the mean strain effect on fatigue resistance. The probability of fracture P is defined below (5) per ASM handbook (Ref 6):

$$P = \frac{(3r - 1)}{(3n + 1)} \times 100\% \quad \text{(Eq 5)}$$

where n is the totaling number of tested specimens, and r is the number of fractured specimens at a particular strain level. The comparison of P for different mean strains and strain amplitudes is plotted in Fig. 5. The P values listed in Table 4 show no difference for mean strain between 2.0 and 4.0%.

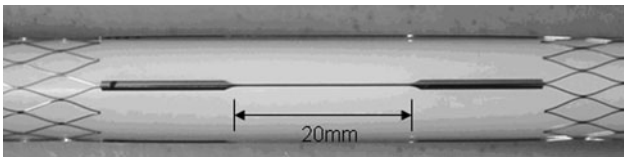

Fig. 1 The dog-bone stent cage: four dog-bone style specimens are cut from a single nitinol hypotube. Specimens are spaced 90

Table 1 Average strut/gauge width and thickness of dog-bone style specimens measured at three locations in the gage in 20 of 80 fatigue specimens

Strut/gauge width	281 ± 9 μm	C.V. = 3.2%
Strut thickness	203 ± 5 μm	C.V. = 2.5%

C.V. stands for coefficient of variation. $N = 20$

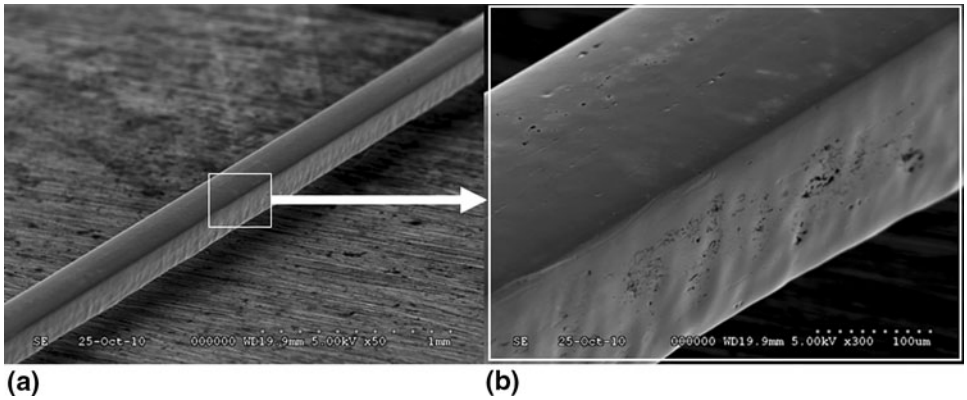

Fig. 2 The dog-bone specimen in the gage section: (a) overall surface finish; and (b) close-up of the electropolished surface. The scallop-like surface on side-wall is the evidence of laser-cutting

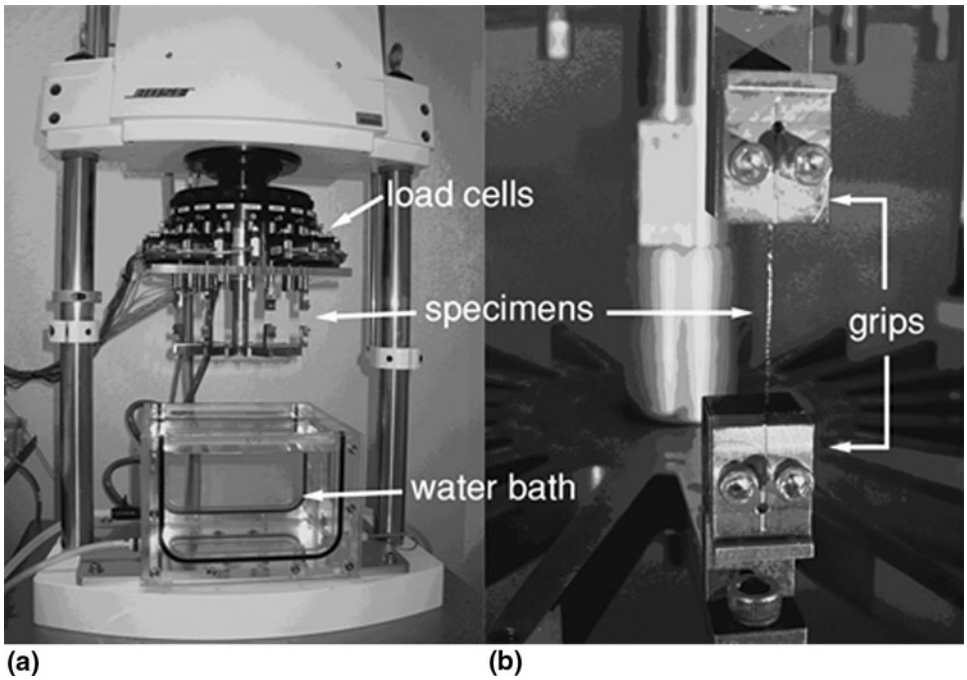

Fig. 3 The overall test setup with load cells on each upper grip for each individual specimen (a), close-up of the grips and the dog-bone style specimen (b)

Table 2 Matrix for mean strain and strain amplitude as well as the testing strain range

ε_m, %	ε_a, %	ε_{max}, %	ε_{min}, %	Replicate *n*
4	1.25	2.75	5.25	4
	1.00	3.00	5.00	5
	0.75	3.25	4.75	5
	0.50	3.50	4.50	10
	0.25	3.75	4.25	5
2	1.25	0.75	3.25	4
	1.00	1.00	3.00	5
	0.75	1.25	2.75	5
	0.50	1.50	2.50	10
1	1.00	0.00	2.00	5
	0.75	0.25	1.75	13
	0.50	0.50	1.50	9

The *P* values at a mean strain of 1.0% appear to be the lowest compared to those at mean strains of 2.0 and 4.0%, which indicates that the dog-bone specimens have the best fatigue resistance at the mean strain of 1.0%.

4. Discussions

The peak and valley values for both stress and strain during the fatigue test are overlaid on a cyclic stress-strain curve in Fig. 6. The cyclic stress-strain curve was the first stress-strain cycle and recorded using the Bose fatigue tester with a cycling speed of 1 Hz and a cycling strain ranging from 0 to 6%. Three groups of fatigue data (ε_m = 1.0, 2.0, and 4.0%) with peak and valley values for both stress and strain are presented in the figure. The strain amplitude for all the three groups was the same at 0.75%. For the mean strain of 1.0%, a dog-bone specimen appeared to be cycling within elastic deformation of austenitic phase. For the mean strain of either 2.0% or 4.0%, a dog-bone specimen appeared to be cycling in austenite and martensite coexisting phase. It is unclear whether the cycling or fatiguing would change the ratio of the austenite percentage to the martensite percentage.

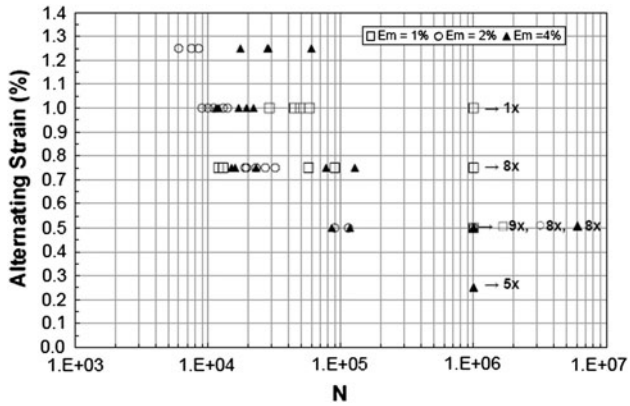

Fig. 4 Fatigue life *N* (dog-bone style specimens) as function of strain amplitude (alternating strain) and mean strain. The arrows show those specimens that ran out at 1E6, and the number shows how many data points are overlapped

As shown in Fig. 5, the probability of fracture values for the strain amplitude of 0.75% were 35, 88, and 88% at mean strains of 1.0, 2.0, and 4.0%, respectively, which indicates that the fatigue resistance is the greatest at 1.0% mean strain. The mean strain effect on fatigue strain limit observed here agrees with what was described in Tabanli's article (Ref 5) that in tension-tension loading, nitinol has better fatigue resistance in its single phase than in its coexisting phases. The dog-bone specimens in

Table 3 List of the raw data of the fatigue test

Specimen No.	ε_m, %	ε_a, %	σ_{valley}, MPa	σ_{Peak}, MPa	Fatigue cycle(a)
1	4.0	1.25	17.14	303.57	28502
2	4.0	1.25	8.04	306.96	60002
3	4.0	1.25	22.32	326.25	28002
4	4.0	1.25	12.32	332.50	17502
5	4.0	1.00	76.25	341.25	11502
6	4.0	1.00	72.14	343.21	12002
7	4.0	1.00	85.00	338.21	19502
8	4.0	1.00	90.00	365.54	17002
9	4.0	1.00	97.68	337.50	22002
10	4.0	0.75	124.64	338.93	127502
11	4.0	0.75	126.96	343.57	77502
12	4.0	0.75	133.04	348.57	16002
13	4.0	0.75	89.29	333.21	23002
14	4.0	0.75	90.36	352.14	15002
15	4.0	0.50	183.75	345.89	85502
16	4.0	0.50	171.61	324.64	1000000
17	4.0	0.50	166.25	310.00	1000000
18	4.0	0.50	176.25	339.46	1000000
19	4.0	0.50	189.64	345.00	1000000
20	4.0	0.50	164.82	321.07	1000000
21	4.0	0.50	166.79	312.50	1000000
22	4.0	0.50	169.11	313.57	1000000
23	4.0	0.50	161.07	313.57	1000000
24	4.0	0.50	161.79	319.64	117002
25	4.0	0.25	238.21	325.71	1000000
26	4.0	0.25	238.04	323.57	1000000
27	4.0	0.25	203.39	278.93	1000000
28	4.0	0.25	256.07	344.46	1000000
29	4.0	0.25	251.25	341.96	1000000
30	2.0	1.25	33.04	360.00	7502
31	2.0	1.25	40.36	362.86	8502
32	2.0	1.25	40.89	370.00	7502
33	2.0	1.25	24.11	380.89	6002
34	2.0	1.00	53.75	333.57	14002
35	2.0	1.00	63.21	361.61	13002
36	2.0	1.00	51.61	367.50	10002
37	2.0	1.00	62.50	356.43	11002
38	2.0	1.00	69.82	390.89	9002
39	2.0	0.75	95.89	351.96	23002
40	2.0	0.75	95.36	333.57	19502
41	2.0	0.75	89.64	318.04	32002
42	2.0	0.75	110.00	369.11	19002
43	2.0	0.75	102.14	328.04	27002
44	2.0	0.50	166.61	337.32	1000000
45	2.0	0.50	174.29	334.11	1000000
46	2.0	0.50	171.61	336.96	1000000
47	2.0	0.50	175.54	349.11	1000000
48	2.0	0.50	191.25	356.61	1000000
49	2.0	0.50	153.75	302.68	1000000
50	2.0	0.50	164.11	329.11	1000000
51	2.0	0.50	165.18	329.82	90002
52	2.0	0.50	169.11	345.89	114002
53	2.0	0.50	147.14	299.82	1000000
54	1.0	1.00	−1.07	325.71	1000000
55	1.0	1.00	−5.36	349.29	49502
56	1.0	1.00	−6.61	357.86	44502
57	1.0	1.00	−2.68	385.89	29002
58	1.0	1.00	−6.61	332.68	58002
59	1.0	0.75	50.54	329.82	1000000
60	1.0	0.75	50.54	313.39	1000000
61	1.0	0.75	51.43	318.75	1000000
62	1.0	0.75	41.07	339.82	1000000
63	1.0	0.75	39.46	329.29	1000000
64	1.0	0.75	111.07	355.89	13002
65	1.0	0.75	107.50	343.39	90002
66	1.0	0.75	68.04	306.43	57002
67	1.0	0.75	81.96	347.50	12002
68	1.0	0.75	104.29	351.43	12002
69	1.0	0.75	37.86	313.04	1000000
70	1.0	0.75	41.79	290.18	1000000
71	1.0	0.75	37.14	296.25	1000000
72	1.0	0.50	103.39	277.68	1000000
73	1.0	0.50	94.64	262.14	1000000
74	1.0	0.50	92.32	262.14	1000000
75	1.0	0.50	99.46	291.79	1000000
76	1.0	0.50	103.93	296.43	1000000
77	1.0	0.50	104.29	286.61	1000000
78	1.0	0.50	111.43	300.71	1000000
79	1.0	0.50	80.54	274.11	1000000
80	1.0	0.50	107.32	294.11	1000000

(a) The 1,000,000 is run-out, and the tested specimen survives. The entire fracture was located at the gage section, and there was one fracture per fatigue failure specimen

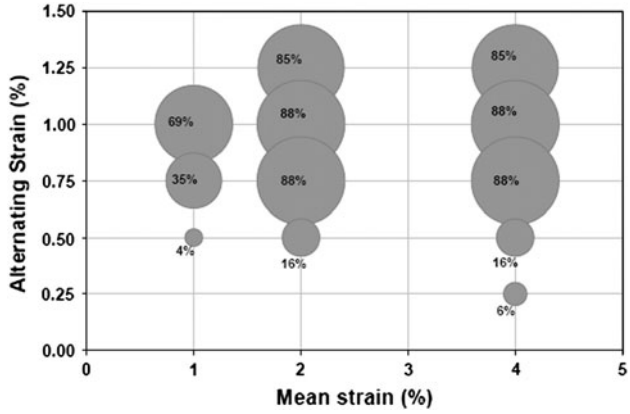

Fig. 5 The probability of fracture *P* (the percentage in or near each circle) shown as a function of strain amplitude (alternating strain) and mean strain

Table 4 List of the calculated values of Probability of fracture

ε_m, %	ε_a, %	*n*	*r*	*P*, %
4.0	1.25	4	4	85
	1.00	5	5	88
	0.75	5	5	88
	0.50	10	2	16
	0.25	5	0	6
2.0	1.25	4	4	85
	1.00	5	5	88
	0.75	5	5	88
	0.50	10	2	16
1.0	1.00	5	4	69
	0.75	13	5	35
	0.50	9	0	4

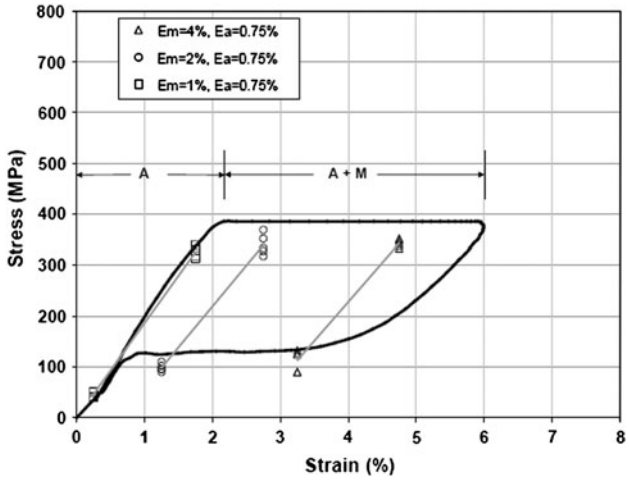

Fig. 6 Maximum and minimum of stresses and strains from three groups of data: mean strain at 1, 2, and 4% are overlaid on a stress-strain curve. The dark line is a stress-strain curve at a cyclic frequency of 1 Hz. The stress-strain curve was collected using the Bose fatigue tester

this study demonstrate much better fatigue resistance than the tubing specimens studied in Tabanli's article. The surface finish and specimen mass likely contribute to the difference. The smoother surface finish on dog-bone specimens lowers the probability of failure due to surface cracks. The small volume of the specimen used in this study would mean that less latent heat is generated during testing if the alternating stress causes stress-inducing martensite. Since latent heat could warm the specimen locally, it would increase the temperature gap between specimen temperature and the specimen A_f. The researchers in their study (Ref 7) have claimed that a larger gap temperature will lower a specimen's fatigue resistance.

The testing results obtained when using a tension-tension method with dog-bone specimens show an opposite mean strain effect compared to those obtained when using a bending method with V-shaped specimens (Ref 2). Pelton et al. (Ref 3) investigated nitinol bending fatigue using diamond style specimen and claimed "that the nitinol diamond-shaped specimens have a constant fatigue life with a strain amplitude of ±0.4% up to an applied mean strain of approximately 1.5%. Above a mean strain of 1.5%, the fatigue life appears to increase with increasing mean strain, strongly indicating that

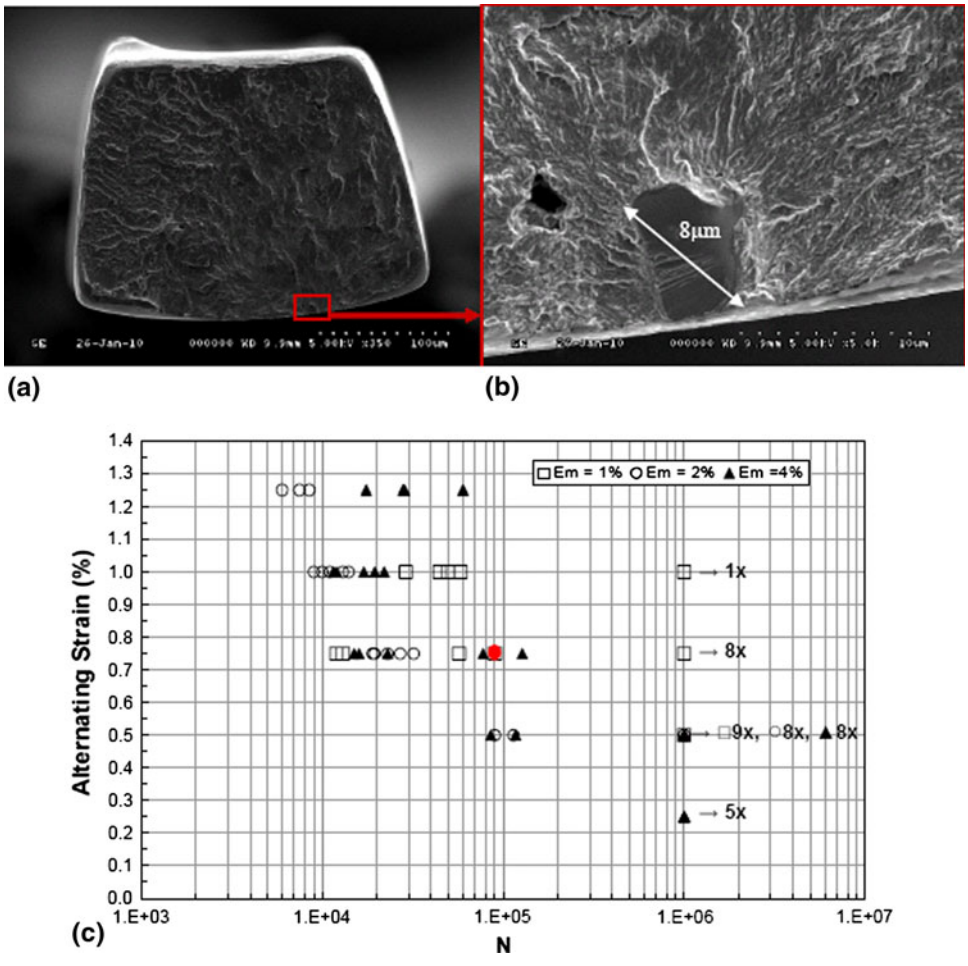

Fig. 7 A fracture surface of a premature failure specimen: (a) The open square indicates the crack initiation area, (b) The close-up of the crack initiation area, and the polygon with darker contrast as an inclusion with a diagonal dimension of 8 μm, (c) A solid dot shows the location of the fatigue specimen on the S-N plot. Eight specimens ran out at 1E6 at the 0.75% strain amplitude (alternating strain)

Table 5 Summary of failure analysis on fractured specimens that are outliers of the group

Mean strain ε_m, %	Strain amplitude ε_a, %	Survived sample *n-r*	Fractured sample *r*	Inclusion at crack initiation
4.0	0.50	8	2	2
2.0	0.50	8	2	2
1.0	0.75	8	5	4(a)

(a) One specimen is excluded because the fracture surfaces suffered additional damage post fracture

Table 6 List of the calculated values of Probability of fracture (for excluded specimens that have been found with an inclusion at crack initiation)

ε_m, %	ε_a, %	*n*	*r*	*P*, %
4.0	1.25	4	4	85
	1.00	5	5	88
	0.75	5	5	88
	0.50	8	0	4
	0.25	5	0	6
2.0	1.25	4	4	85
	1.00	5	5	88
	0.75	5	5	88
	0.50	8	0	4
1.0	1.00	5	4	69
	0.75	9	1	7
	0.50	9	0	4

the formation of stress-induced martensite is responsible for this desirable behavior." In this fatigue study with dog-bone specimen, the fatigue specimen was in the coexisting phase when mean strain was at 2% or 4%. However, there were no data from this study to support the view whether the ratio of martensite to austenite was changing during the fatigue test. The specimens in the coexisting phase exhibit fatigue resistance that trends worse than specimens remaining in single phase in tension-tension test. The fatigue behavior difference between dog-bone and V-shaped specimens may be due to the difference in strain distribution. Strain distribution on tension-tension dog-bone specimen is uniform across the gage length, whereas that in a V- or diamond-shaped specimen has gradient.

Inclusions in this nitinol fatigue study also impact the specimen fatigue resistance. As shown in Fig. 4, the results of fatigue resistance are in bi-modal for the following strain combinations:

1. mean strain ε_m = 4.0%, and strain amplitude ε_a = 0.5%
2. mean strain ε_m = 2.0%, and strain amplitude ε_a = 0.5%
3. mean strain ε_m = 1.0%, and strain amplitude ε_a = 0.75%

In these strain settings, most specimens tested survived the fatigue test, but 20-40% of the tested specimens in these groups fractured prematurely. Scanning electron microscopy (SEM) was used to examine the fracture surfaces of the specimens. Crack initiation was indentified for all the nine prematurely fractured specimens. Eight of the nine specimens show an inclusion at the crack initiation area as shown in Fig. 7. These inclusions have very similar characteristic: polygon shape with a diagonal dimension around 5-8 μm. The failure analysis was indeterminate on one specimen with premature failure because the fracture surfaces suffered additional damage post fracture. The summary of SEM examination is given in Table 5. The bimodal effect happens only at certain strain levels. It suggests that the effect may be relative to the size of the inclusion. If specimens that have been found with an inclusion at crack initiation are excluded, then the bimodal effect disappears as shown in Table 6.

5. Conclusions

In tension-tension fatigue, the fatigue strain limits at 10^6 cycles for dog-bone style specimen with a stent quality finish are as follows:

mean strain ε_m = 4.0% and strain amplitude ε_a = 0.25%
mean strain ε_m = 1.0% and strain amplitude ε_a = 0.5%

If the inclusion effect is excluded, the fatigue strain limits at 10^6 cycles for dog-bone style specimen with a stent quality finish could be as follows:

mean strain ε_m = 4.0% and strain amplitude ε_a = 0.5%
mean strain ε_m = 2.0% and strain amplitude ε_a = 0.5%
mean strain ε_m = 1.0% and strain amplitude ε_a = 0.75%

For tension-tension fatigue, the dog-bone style specimens have better fatigue resistance when the loading stays in single phase regime as opposed to loading that includes mixed phases.

Acknowledgments

This study was conducted as part of research in progress of a consortium of several stent manufacturers, such as SAFE Technology Limited and Dassault Systèmes Simulia Corporation, which are committed to the development of improved life prediction of nitinol devices. The fatigue data in this study are part of the consortium database which will be used to produce a damage curve assessment life prediction for nitinol.

References

1. D. Stoeckel, Nitinol Medical Devices and Implants, *Min. Invas. Ther. Allied Technol.*, 2000, **9**(3), p 81–88
2. W.J. Harrison and Z.C. Lin, *Proceedings of the International Conference on Shape Memory and Superelastic Technologies*, S.M. Russell and A.R. Pelton, Ed., April 30-May 3, 2000, Pacific Grove, California, 2000, p 391–396
3. A.R. Pelton, V. Schroeder, M.R. Mitchell, X.-Y. Gong, M. Barney, and S.W. Robertson, Fatigue and Durability of Nitinol Stents, *J. Mech. Behav. Biomed. Mater.*, 2008, **I**, p 153–164
4. S. Wong, Z.C. Lin, A. Tahran, J. Boylan, K. Pike, and P. Kramer-Brown, An Investigation of Factors Impacting Nitinol Wire Fatigue Life, *J. ASTM Int.*, **6**(8), p 99–107. doi:10.1520/JAI102195
5. R.M. Tabanli, N.K. Simha, and B.T. Berg, Mean Strain Effect on the Fatigue Properties of Superelastic NiTi, *Metall. Mater. Trans. A*, 2001, **32A**, p 1866–1869
6. ASM Handbook, Vol 19: Fatigue and Fracture, 1996, ASM International, p 305
7. Y.S. Kim and S. Miyazaki, *Proceedings of the International Conference on Shape Memory and Superelastic Technologies*, A. Pelton, D. Hodgson, S. Russell, and T. Duerig, Ed., March 2–6, 1997, Pacific Grove, California, 1997, p 473–478